

Low-Dimensional Ferromagnetic Properties of SrCuV<sub>2</sub>O<sub>7</sub> and BaCuV<sub>2</sub>O<sub>7</sub>Alexei A. Belik,<sup>\*†‡</sup> Masaki Azuma,<sup>†‡</sup> Akira Matsuo,<sup>§</sup> Koichi Kindo,<sup>§</sup> and Mikio Takano<sup>†</sup>*Institute for Chemical Research, Kyoto University, Uji, Kyoto-fu 611-0011, Japan, PRESTO, Japan Science and Technology Agency (JST), Kawaguchi, Saitama 332-0012, Japan, and KYOKUKEN, Osaka University, Toyonaka, Osaka 560-8531, Japan*

Received January 31, 2005

The crystal structure of isostructural SrCuV<sub>2</sub>O<sub>7</sub> and BaCuV<sub>2</sub>O<sub>7</sub> consists of one-dimensional (1D) zigzag chains of Cu atoms with next-nearest-neighbor interaction. The main intrachain interaction was found to be ferromagnetic and estimated at 4.6 K (Hamiltonian  $H \sim -2J$ ). SrCuV<sub>2</sub>O<sub>7</sub> and BaCuV<sub>2</sub>O<sub>7</sub> are new examples in the scanty family of 1D ferromagnets. Isothermal magnetization measurements at 0.08 K and specific heat data showed that MCuV<sub>2</sub>O<sub>7</sub> exhibits antiferromagnetic long-range ordering at  $T_N = 1.36$  K for SrCuV<sub>2</sub>O<sub>7</sub> and  $T_N = 1.47$  K for BaCuV<sub>2</sub>O<sub>7</sub>. Spin-flop transitions were observed in the antiferromagnetic state at 0.08 K near 0.5 kOe in SrCuV<sub>2</sub>O<sub>7</sub> and 2 kOe in BaCuV<sub>2</sub>O<sub>7</sub>. In air, SrCuV<sub>2</sub>O<sub>7</sub> and BaCuV<sub>2</sub>O<sub>7</sub> melted incongruently above 983 and 1018 K, respectively.

## 1. Introduction

The properties of low-dimensional magnets continue to be of great interest to physicists and chemists.<sup>1</sup> One of the reasons for such interest is to understand superconducting properties of the two-dimensional copper oxides. Of the many possible combinations of dimensionality and spin quantum number ( $S$ ), one combination which has been conspicuous by the lack of realizations is the one-dimensional (1D)  $S = 1/2$  Heisenberg ferromagnet.<sup>2–4</sup> The numerous studies on 1D magnetic systems have been on antiferromagnets, for example,  $S = 5/2$  Heisenberg (Mn<sup>2+</sup>),  $S = 1$  (Ni<sup>2+</sup>, Haldane system),  $S = 1/2$  Ising (Co<sup>2+</sup>), and  $S = 1/2$  Heisenberg (Cu<sup>2+</sup>) systems. However, there are only few examples of the 1D  $S = 1/2$  Heisenberg ferromagnets, for example, (CH<sub>3</sub>)NCuCl<sub>3</sub>,<sup>2</sup> [(CH<sub>3</sub>)NH]<sub>3</sub>Cu<sub>2</sub>Cl<sub>7</sub>,<sup>2</sup> K<sub>2</sub>Cu<sub>0.59</sub>Zn<sub>0.41</sub>F<sub>4</sub> (diluted two-dimensional ferromagnet),<sup>5</sup> some organic radical compounds,<sup>3,4,6</sup> and the most studied (C<sub>6</sub>H<sub>11</sub>NH<sub>3</sub>)CuBr<sub>3</sub> and (C<sub>6</sub>H<sub>11</sub>NH<sub>3</sub>)-

CuCl<sub>3</sub>.<sup>7–9</sup> The 1D  $S = 1/2$  Ising ferromagnets are presented, for example, by CoCl<sub>2</sub>\*2H<sub>2</sub>O, CoBr<sub>2</sub>\*2H<sub>2</sub>O, RbFeCl<sub>3</sub>\*2H<sub>2</sub>O, and CoCl<sub>2</sub>(NC<sub>3</sub>H<sub>5</sub>)<sub>2</sub>.<sup>7</sup>

1D ferromagnets are particularly of interest because quantum effects are expected to be most pronounced in them. The anisotropies of  $J$  values (Ising-type contribution), even if they are very small, give rise to a qualitative change in the thermodynamical quantities, especially in an applied field, for 1D ferromagnets in comparison with 1D antiferromagnets.<sup>2,3,9</sup> Theoretically, the 1D  $S = 1/2$  Heisenberg ferromagnet has been investigated a lot.<sup>10–12</sup> However, the comparison of theory and experiments is restricted by a very small number of the 1D  $S = 1/2$  Heisenberg ferromagnets.

Magnetic sublattice in two isostructural compounds SrCuV<sub>2</sub>O<sub>7</sub> (space group  $Pnma$ ,  $a = 14.470$  Å,  $b = 5.4704$  Å, and  $c = 7.4201$  Å)<sup>13</sup> and BaCuV<sub>2</sub>O<sub>7</sub>,<sup>14</sup> whose magnetic properties have not been investigated yet, can be presented, from the structural point of view, by a model of the double chain or by a model of the uniform zigzag chain with next-

\* Author to whom correspondence should be addressed. Present address: International Center for Young Scientists, National Institute for Materials Science, Namiki 1-1, Tsukuba, Ibaraki, 305-0044, Japan. E-mail: Alexei.BELIK@nims.go.jp.

† Kyoto University.

‡ Japan Science and Technology Agency.

§ Osaka University.

- (1) Lemmens, P.; Güntherodt, G.; Gros, C. *Phys. Rep.* **2003**, *375*, 1.
- (2) Landee, C. P.; Willett, R. D. *Phys. Rev. Lett.* **1979**, *43*, 463.
- (3) Takeda, K.; Konishi, K.; Nedachi, K.; Mukai, K. *Phys. Rev. Lett.* **1995**, *74*, 1673.
- (4) Mukai, K.; Suzuki, K.; Ohara, K.; Jamali, J. B.; Achiwa, N. *J. Phys. Soc. Jpn.* **1999**, *68*, 3078.
- (5) Takeda, K.; Okuda, Y.; Yamada, I.; Haseda, T. *J. Phys. Soc. Jpn.* **1981**, *50*, 1917.
- (6) Takeda, K.; Hamano, T.; Kawae, T.; Hidaka, M.; Takahashi, M.; Kawasaki, S.; Mukai, K. *J. Phys. Soc. Jpn.* **1995**, *64*, 2343.

- (7) Haines, D. N.; Drumheller, J. E. *Phys. Rev. Lett.* **1987**, *58*, 2702.
- (8) Kopinga, K.; Delica, T.; Leschke, H.; Riedel, I. *Phys. Rev. B* **1993**, *47*, 5447.
- (9) Campana, L. S.; Caramico D'Auria, A.; Esposito, U.; Kamieniarz, G. *Phys. Rev. B* **1990**, *41*, 6733.
- (10) Bonner, J. C.; Fisher, M. E. *Phys. Rev. A* **1964**, *135*, 640.
- (11) Johnson, J. D.; Bonner, J. C. *Phys. Rev. B* **1980**, *22*, 251.
- (12) Takahashi, M.; Turek, P.; Nakazawa, Y.; Tamura, M.; Nozawa, K.; Shiomo, D.; Ishikawa, M.; Kinoshita, M. *Phys. Rev. Lett.* **1991**, *67*, 746.
- (13) Vogt, R.; Mueller-Buschbaum, H. Z. *Anorg. Allg. Chem.* **1991**, *594*, 127.
- (14) Vogt, R.; Mueller-Buschbaum, H. *J. Less-Common Met.* **1991**, *171*, 35.

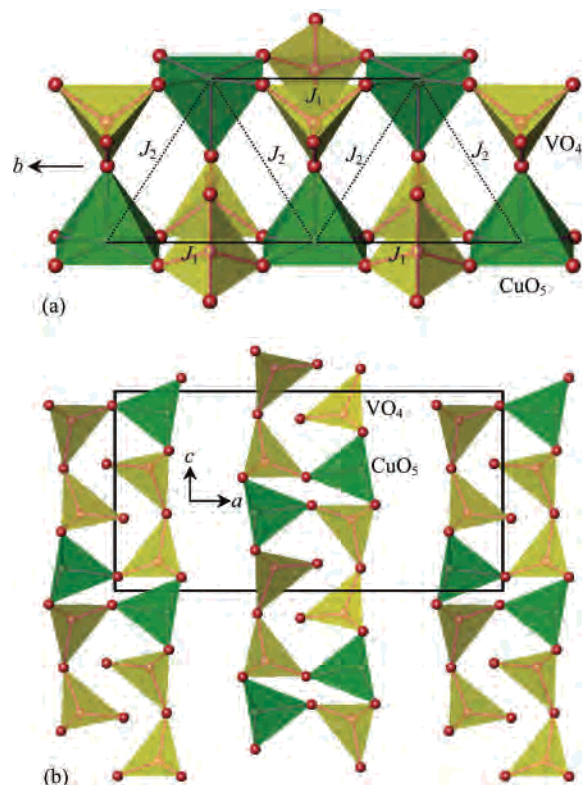


**Figure 1.** (a) The double Cu chain in  $\text{SrCuV}_2\text{O}_7$  along the  $b$  axis (or uniform zigzag chain with next-nearest-neighbor interaction). (b) The arrangement of the double Cu chains in the crystal structure of  $\text{SrCuV}_2\text{O}_7$ : projection along the  $b$  axis.

nearest-neighbor (NNN) interaction<sup>15</sup> (Figure 1a) along the  $b$  axis (Figure 1b). These models are described by two exchange constants,  $J_1$  and  $J_2$ . There is one Cu site in  $\text{MCuV}_2\text{O}_7$  ( $M = \text{Sr}$  and  $\text{Ba}$ ), and the Cu atom has a square pyramidal coordination. The Cu atoms are connected with each other through super-superexchange interactions<sup>16</sup> including two  $\text{Cu}-\text{O}\cdots\text{O}-\text{Cu}$  paths, where the  $\text{O}\cdots\text{O}$  is an edge of  $\text{VO}_4$  groups (Figure 1a). The basal planes of the  $\text{CuO}_5$  pyramids lie on one plane and the  $\text{Cu}-\text{O}\cdots\text{O}$  angles are  $134.3^\circ$  and  $134.6^\circ$  (for  $\text{SrCuV}_2\text{O}_7$ ). Such a type of connection between magnetic ions usually gives rather strong antiferromagnetic interaction ( $J_1 \sim -50$  K, Hamiltonian  $H = -2J_1\sum_i S_i S_{i+1}$ ).<sup>17</sup> On the other hand, the connection between Cu atoms responsible for  $J_2$  includes long apical  $\text{Cu}-\text{O}$  bonds (Figure 1a), and one of the  $\text{Cu}-\text{O}\cdots\text{O}$  angles ( $149.3^\circ$  and  $98.0^\circ$  for  $\text{SrCuV}_2\text{O}_7$ ) is close to  $90^\circ$ .  $J_2$  was therefore expected to be very small. As a result, we expected vanadates  $\text{MCuV}_2\text{O}_7$  ( $M = \text{Sr}$  and  $\text{Ba}$ ) to be simple uniform 1D  $S = 1/2$  linear chain Heisenberg antiferromagnets such as phosphates  $\text{SrCuP}_2\text{O}_7$ <sup>17</sup> and  $\text{BaCuP}_2\text{O}_7$ .<sup>18</sup> However, phosphates  $\text{SrCuP}_2\text{O}_7$  and  $\text{BaCuP}_2\text{O}_7$  have different crystal structures in comparison with vanadates  $\text{MCuV}_2\text{O}_7$  ( $M = \text{Sr}$  and  $\text{Ba}$ ).

Surprisingly, magnetic properties of  $\text{MCuV}_2\text{O}_7$  ( $M = \text{Sr}$  and  $\text{Ba}$ ) resembled those observed for the 1D  $S = 1/2$

Heisenberg ferromagnets. In This Paper, we present the results of specific heat and dc and ac magnetization measurements in different static magnetic fields. These results evidence on the 1D ferromagnetic properties of  $\text{MCuV}_2\text{O}_7$  ( $M = \text{Sr}$  and  $\text{Ba}$ ).  $\text{SrCuV}_2\text{O}_7$  and  $\text{BaCuV}_2\text{O}_7$  are new examples in the scanty family of the 1D  $S = 1/2$  ferromagnets.

## 2. Experimental Section

**Synthesis.**  $\text{SrCuV}_2\text{O}_7$ ,  $\text{BaCuV}_2\text{O}_7$ , and  $\text{BaZnV}_2\text{O}_7$  were synthesized from stoichiometric mixtures of  $\text{SrCO}_3$  (99.99%),  $\text{BaCO}_3$  (99.99%),  $\text{CuO}$  (99.9%),  $\text{ZnO}$  (99.99%), and  $\text{V}_2\text{O}_5$  (99.8%) by the solid-state method. The mixtures were pressed into pellets and allowed to react at 943 K ( $\text{SrCuV}_2\text{O}_7$  and  $\text{BaCuV}_2\text{O}_7$ ) and 873 K ( $\text{BaZnV}_2\text{O}_7$ )<sup>19</sup> for 200 h with four intermediate grindings on Pt plates. X-ray powder diffraction (XRD) data collected with a RIGAKU RINT 2500 diffractometer ( $2\theta$  range of  $5-60^\circ$ , a step width of  $0.02^\circ$ , and a counting time of 1 s/step) showed that the three samples were monophasic.  $\text{SrCuV}_2\text{O}_7$  and  $\text{BaCuV}_2\text{O}_7$  were khaki green and  $\text{BaZnV}_2\text{O}_7$  was pink.  $\text{BaZnV}_2\text{O}_7$  is isotopic<sup>19</sup> with  $\text{BaCuV}_2\text{O}_7$  and can be used to estimate the lattice contribution in the specific heat.  $\text{SrZnV}_2\text{O}_7$  crystallizes, however, in a different structure type (space group  $P2_1/n$ ).<sup>20</sup>

**Magnetic and Specific Heat Measurements.** Direct current (dc) magnetic susceptibility ( $\chi = M/H$ ) was measured on a Quantum Design SQUID magnetometer (MPMS XL) between 2 and 300 K in an applied field of 100 Oe under both zero-field-cooled (ZFC) and field-cooled (FC) conditions. Isothermal magnetization curves were recorded between  $-50$  and  $+50$  kOe at 2, 3, 4, 5, 10, and 15 K. Magnetization data at 0.08 K were taken in a pulsed magnetic field up to 150 kOe by an induction method using a multilayer pulse magnet at KYOKUGEN, Osaka University. Alternating current (ac) susceptibility measurements were performed with a Quantum Design PPMS instrument in the temperature range of 1.8–30 K (on cooling) at frequencies ( $f$ ) of 10,  $10^2$ ,  $5 \times 10^2$ , and  $10^3$  Hz, applied oscillating magnetic field ( $H_{ac}$ ) of 1 Oe, and different static magnetic fields ( $H_{dc}$ ) ranging from 0 to 20 kOe. Specific heat,  $C_p$  versus  $T$ , of  $\text{SrCuV}_2\text{O}_7$  and  $\text{BaCuV}_2\text{O}_7$  was recorded between 0.45 and 300 K (between 1.8 and 170 K for  $\text{BaZnV}_2\text{O}_7$ ) on cooling at zero magnetic field by a pulse relaxation method using a commercial calorimeter (Quantum Design PPMS). At magnetic fields of 5, 10, 30, 50, and 90 kOe, the  $C_p$  versus  $T$  data were taken between 2 and 21 K for  $\text{SrCuV}_2\text{O}_7$  and  $\text{BaCuV}_2\text{O}_7$ .

**Thermal Analysis.** Thermal stability of  $\text{SrCuV}_2\text{O}_7$ ,  $\text{BaCuV}_2\text{O}_7$ , and  $\text{BaZnV}_2\text{O}_7$  was examined under air with a MacScience TG-DTA 2000 instrument. The samples were placed in Pt crucibles, heated, and then cooled with a rate of 10 K/min.  $\text{SrCuV}_2\text{O}_7$  was heated to 1013 K,  $\text{BaCuV}_2\text{O}_7$  up to 1058 K, and  $\text{BaZnV}_2\text{O}_7$  up to 1073 K. Differential thermal analysis (DTA) showed peaks at 993 and 998 K on heating and at 976 and 917 K on cooling for  $\text{SrCuV}_2\text{O}_7$ ; at 1029, 1033, and 1047 K on heating and a very broad peak at 887 K on cooling for  $\text{BaCuV}_2\text{O}_7$ ; and at 1047 K on heating and broad peaks at 978 and 905 K on cooling for  $\text{BaZnV}_2\text{O}_7$ . Such inconsistency of heating and cooling behavior suggests that  $\text{SrCuV}_2\text{O}_7$ ,  $\text{BaCuV}_2\text{O}_7$ , and  $\text{BaZnV}_2\text{O}_7$  melt incongruently above 983, 1018, and 1033 K, respectively. No structural phase transition was detected by DTA in  $\text{BaZnV}_2\text{O}_7$  at 943 K.<sup>19</sup>

(15) Maeshima, N.; Okunishi, K. *Phys. Rev. B* **2000**, *62*, 934.

(16) Whangbo, M.-H.; Koo, H.-J.; Dai, D.; Jung, D. *Inorg. Chem.* **2003**, *42*, 3898.

(17) Belik, A. A.; Azuma, M.; Takano, M. *Inorg. Chem.* **2003**, *42*, 8572.

(18) Belik, A. A.; Azuma, M.; Takano, M. *J. Magn. Magn. Mater.* **2004**, *272–276*, 937.

(19) International Centre for Diffraction Data. Powder Diffraction File No. 46-0759.

(20) Velikodnyi, Yu. A.; Myrashova, E. V.; Trunov, V. K. *Kristallografiya* **1989**, *34*, 607.

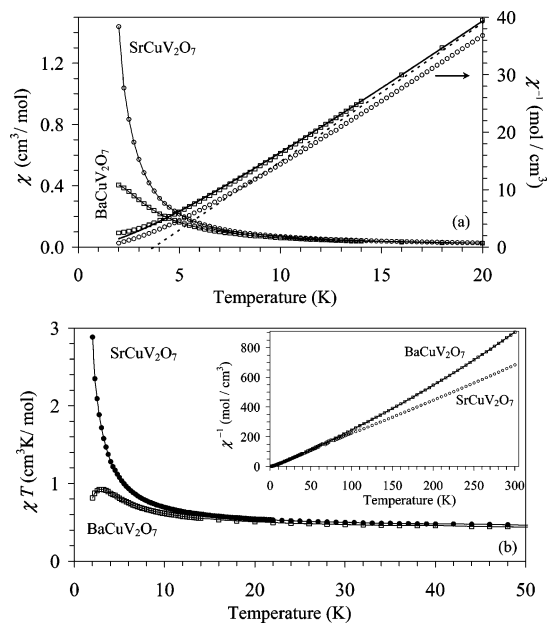


**Figure 2.** (a) The  $\chi$  vs  $T$  (symbols with line) and  $\chi^{-1}$  vs  $T$  (symbols) curves measured at 100 Oe for SrCuV<sub>2</sub>O<sub>7</sub> and BaCuV<sub>2</sub>O<sub>7</sub>. The solid line for the  $\chi^{-1}$  vs  $T$  curve shows the fit to eq 2 and the dashed line presents the fit to eq 1 for BaCuV<sub>2</sub>O<sub>7</sub> as an example. (b) The  $\chi T$  vs  $T$  curves between 2 and 50 K for SrCuV<sub>2</sub>O<sub>7</sub> and BaCuV<sub>2</sub>O<sub>7</sub>. Inset gives the  $\chi^{-1}$  vs  $T$  curves for SrCuV<sub>2</sub>O<sub>7</sub> and BaCuV<sub>2</sub>O<sub>7</sub> between 2 and 300 K with the Curie–Weiss fit for BaCuV<sub>2</sub>O<sub>7</sub>.

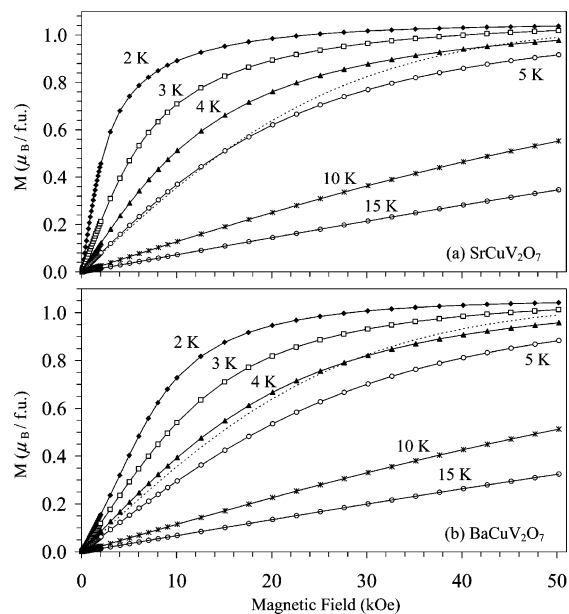
### 3. Results and Discussion

Figure 2a depicts the  $\chi$  versus  $T$  and  $\chi^{-1}$  versus  $T$  curves for SrCuV<sub>2</sub>O<sub>7</sub> and BaCuV<sub>2</sub>O<sub>7</sub>. No noticeable difference was found between the ZFC and FC curves. The  $\chi$  versus  $T$  curves showed no broad maxima characteristic of low-dimensional antiferromagnets. The  $\chi$  values increased with decreasing temperature in the whole temperature range of 2–300 K. Thus, SrCuV<sub>2</sub>O<sub>7</sub> and BaCuV<sub>2</sub>O<sub>7</sub> are not low-dimensional antiferromagnets. The  $\chi^{-1}$  versus  $T$  data at 15–300 K were fitted by a modified Curie–Weiss expression

$$\chi(T) = \chi_0 + C/(T - \theta) \quad (1)$$

with temperature independent term  $\chi_0 = -6(7) \times 10^{-6}$  cm<sup>3</sup>/mol, Curie constant  $C = 0.440(2)$  cm<sup>3</sup>K/mol, and Weiss constant  $\theta = 3.4(2)$  K for SrCuV<sub>2</sub>O<sub>7</sub> and  $\chi_0 = -3.17(2) \times 10^{-4}$  cm<sup>3</sup>/mol,  $C = 0.4219(5)$  cm<sup>3</sup>K/mol, and  $\theta = 3.75(7)$  K for BaCuV<sub>2</sub>O<sub>7</sub>. The positive Weiss constant indicates that the main interaction between Cu atoms is ferromagnetic. Below about 15 K, the  $\chi^{-1}$  versus  $T$  curves deviated from the Curie–Weiss law. The similar behavior of the  $\chi^{-1}$  versus  $T$  curves was observed in other 1D ferromagnets.<sup>3,4,12</sup> The  $\chi T$  versus  $T$  curve for SrCuV<sub>2</sub>O<sub>7</sub> demonstrated the sharp increase at low-temperature region while the  $\chi T$  versus  $T$  curve for BaCuV<sub>2</sub>O<sub>7</sub> exhibited a broad maximum at 3 K (Figure 2b). Taking into account the structural features of SrCuV<sub>2</sub>O<sub>7</sub> and BaCuV<sub>2</sub>O<sub>7</sub>, the positive Weiss constants are the first indication that SrCuV<sub>2</sub>O<sub>7</sub> and BaCuV<sub>2</sub>O<sub>7</sub> are a 1D  $S = 1/2$  ferromagnetic system.

To roughly estimate the main intrachain interaction, we used the model of the uniform 1D  $S = 1/2$  Heisenberg



**Figure 3.** Isothermal magnetization curves,  $M$  vs  $H$ , at 2, 3, 4, 5, 10, and 15 K for (a) SrCuV<sub>2</sub>O<sub>7</sub> and (b) BaCuV<sub>2</sub>O<sub>7</sub>. The dotted lines are the  $S = 1/2$  Brillouin function with  $g = 2.1$  at 2 K.

ferromagnet,<sup>3,4</sup> that is, assuming that  $J_1$  is dominant ( $J_1 \gg J_2$ ) or  $J_2$  is dominant ( $J_2 \gg J_1$ )

$$\chi(T) = \chi_0 + \frac{Ng^2\mu_B^2}{4k_B T} \left[ 1 + \left( \frac{J_1}{k_B T} \right) \right] \quad (2)$$

where  $N$  is Avogadro's number,  $g$  is the spectroscopic splitting factor ( $g$ -factor),  $\mu_B$  is the Bohr magneton, and  $k_B$  is Boltzmann's constant. Equation 2 is valid for  $k_B T/J_1 > 1$ . The fitting of the  $\chi^{-1}$  versus  $T$  curves to eq 2 between 5 and 300 K yields  $\chi_0 = 1.0(7) \times 10^{-5}$  cm<sup>3</sup>/mol,  $g = 2.151(5)$ , and  $J_1/k_B = 4.6(2)$  K for SrCuV<sub>2</sub>O<sub>7</sub> and  $\chi_0 = -3.10(1) \times 10^{-4}$  cm<sup>3</sup>/mol,  $g = 2.1131(9)$ , and  $J_1/k_B = 4.58(6)$  K for BaCuV<sub>2</sub>O<sub>7</sub>.

The real part of the ac susceptibility curves,  $\chi'$  versus  $T$ , at zero static magnetic field almost coincided with the dc  $\chi$  versus  $T$  curves measured at 100 Oe. Strong dependence of the  $\chi'$  versus  $T$  curves on static magnetic field,  $H_{dc}$ , was found and a broad maximum appeared on the  $\chi'$  versus  $T$  curves from  $H_{dc} = 2$  kOe for SrCuV<sub>2</sub>O<sub>7</sub> and  $H_{dc} = 10$  kOe for BaCuV<sub>2</sub>O<sub>7</sub>.<sup>7</sup> No noticeable difference was found for the  $\chi'$  versus  $T$  curves measured at different frequencies.

Isothermal magnetization curves are given in Figure 3. No hysteresis was observed on the  $M$  versus  $H$  curves. The saturation of magnetization occurred at about 40 kOe for SrCuV<sub>2</sub>O<sub>7</sub> and 50 kOe for BaCuV<sub>2</sub>O<sub>7</sub> at 2 K. The saturation value of about  $1.05 \mu_B/\text{mol}$  was expected for  $S = 1/2$  and  $g \approx 2.1$ . Such magnetization curves were observed in other 1D  $S = 1/2$  ferromagnets.<sup>2,8,12</sup> The experimental magnetization data for SrCuV<sub>2</sub>O<sub>7</sub> and BaCuV<sub>2</sub>O<sub>7</sub> saturated much faster than expected for the  $S = 1/2$  Brillouin function with  $g = 2.1$  (Figure 3). This fact shows the dominating ferromagnetic interaction between Cu<sup>2+</sup> ions.

Figure 4 depicts the  $M$  versus  $H$  and  $dM/dH$  versus  $H$  curves for SrCuV<sub>2</sub>O<sub>7</sub> and BaCuV<sub>2</sub>O<sub>7</sub> at 0.08 K, that is, below the temperatures of long-range magnetic ordering (see the

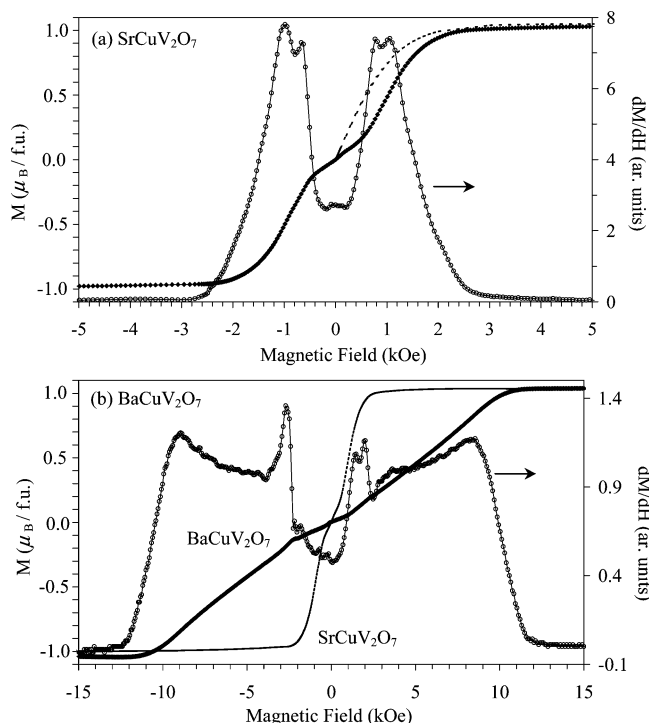


**Figure 4.** (a) The  $M$  vs  $H$  and  $dM/dH$  vs  $H$  curves for SrCuV<sub>2</sub>O<sub>7</sub> at 0.08 K between  $-5$  and  $5$  kOe. The dotted line is the  $S = 1/2$  Brillouin function with  $g = 2.1$  at 0.08 K. (b) The  $M$  vs  $H$  and  $dM/dH$  vs  $H$  curves for BaCuV<sub>2</sub>O<sub>7</sub> at 0.08 K between  $-15$  and  $15$  kOe. The  $M$  vs  $H$  curve for SrCuV<sub>2</sub>O<sub>7</sub> is also shown for comparison.

specific heat data). The saturation magnetization was the same,  $1.05 \mu_B/\text{mol}$ . At low magnetic fields, the magnetization increased linearly with the field and slower than expected for the  $S = 1/2$  Brillouin function with  $g = 2.1$ . No hysteresis was found and the  $M$  versus  $H$  curves passed through the origin. These facts indicate that the 1D ferromagnetic chains are ordered antiferromagnetically in both SrCuV<sub>2</sub>O<sub>7</sub> and BaCuV<sub>2</sub>O<sub>7</sub>. At about 0.5 kOe for SrCuV<sub>2</sub>O<sub>7</sub> and 2 kOe for BaCuV<sub>2</sub>O<sub>7</sub>, the slope change of the  $M$  versus  $H$  curve because of a spin flop transition was detected in the antiferromagnetic state. The small value of the magnetic field for the spin flop transition reflects the very small value of the interchain interaction. The  $dM/dH$  versus  $H$  curve for SrCuV<sub>2</sub>O<sub>7</sub> clearly exhibited two peaks near 0.5 kOe. Thus, two-step spin flop transition is possible.

The  $C_p/T$  versus  $T$  curves for SrCuV<sub>2</sub>O<sub>7</sub>, BaCuV<sub>2</sub>O<sub>7</sub>, and BaZnV<sub>2</sub>O<sub>7</sub> are given in Figure 5a. The  $C_p$  was almost the same in the temperature range of 40–300 K for MCuV<sub>2</sub>O<sub>7</sub> ( $M = \text{Sr}$  and  $\text{Ba}$ ). The  $M$  sublattice seems to give the same constant contribution to the specific heat. This behavior is quite unusual because in the series of isostructural compounds, the heavier atoms give the larger contribution to  $C_p$ .<sup>17,21</sup> On the other hand, the specific heat of BaZnV<sub>2</sub>O<sub>7</sub> was larger than that of BaCuV<sub>2</sub>O<sub>7</sub> in the temperature range of about 13–150 K (Figure 5). This fact shows that the sublattice of the transition-metal ion has a very strong effect on  $C_p$ , that is, even a small change in the mass results in the strong change in  $C_p$ . The estimation of the lattice contribu-

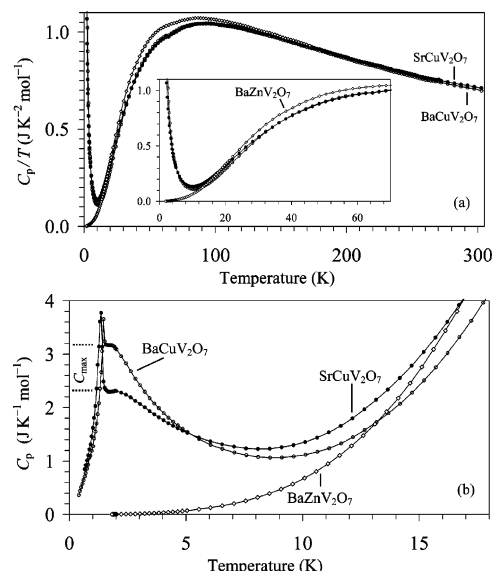


**Figure 5.** (a) Temperature dependence of  $C_p/T$  for SrCuV<sub>2</sub>O<sub>7</sub>, BaCuV<sub>2</sub>O<sub>7</sub>, and BaZnV<sub>2</sub>O<sub>7</sub>. Inset shows the enlarge fragment of the figure. (b) The  $C_p$  vs  $T$  curves up to 18 K for SrCuV<sub>2</sub>O<sub>7</sub>, BaCuV<sub>2</sub>O<sub>7</sub>, and BaZnV<sub>2</sub>O<sub>7</sub>.

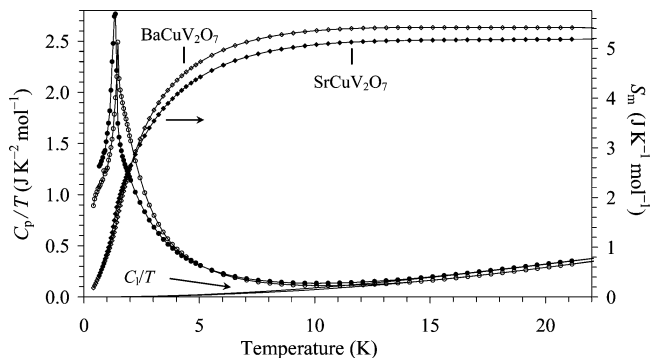


**Figure 6.** The  $C_p/T$  vs  $T$  and  $S_m$  vs  $T$  curves for SrCuV<sub>2</sub>O<sub>7</sub> and BaCuV<sub>2</sub>O<sub>7</sub>. The solid lines show the lattice contribution ( $C_1/T$  vs  $T$  curves).

tion,  $C_1$ , in MCuV<sub>2</sub>O<sub>7</sub> ( $M = \text{Sr}$  and  $\text{Ba}$ ) was therefore not straightforward. The lattice contribution was estimated between 16 and 21 K using the equation

$$C_1 (=C_p) = \beta_1 T^3 + \beta_2 T^5 \quad (3)$$

with  $\beta_1 = 9.38 \times 10^{-4} \text{ J K}^{-4} \text{ mol}^{-1}$  and  $\beta_2 = -3.56 \times 10^{-7} \text{ J K}^{-6} \text{ mol}^{-1}$  for SrCuV<sub>2</sub>O<sub>7</sub> and  $\beta_1 = 7.21 \times 10^{-4} \text{ J K}^{-4} \text{ mol}^{-1}$  and  $\beta_2 = -3.86 \times 10^{-9} \text{ J K}^{-6} \text{ mol}^{-1}$  for BaCuV<sub>2</sub>O<sub>7</sub>. Then, this equation was extended to the lower temperature region.

The magnetic entropy,  $S_m(T) = \int (C_m/T) dT$ , where  $C_m = C_p - C_1$ , was close to  $R \ln 2 \approx 5.76 \text{ J K}^{-1} \text{ mol}^{-1}$  expected for the  $S = 1/2$  systems ( $5.17 \text{ J K}^{-1} \text{ mol}^{-1}$  for SrCuV<sub>2</sub>O<sub>7</sub> and  $5.42 \text{ J K}^{-1} \text{ mol}^{-1}$  for BaCuV<sub>2</sub>O<sub>7</sub>; Figure 6). This fact gives the support that the estimation of  $C_1$  is reasonable. However, the reduced values of  $S_m$  show that the  $C_1$  was overestimated.

The very large difference in the values of broad maximum,  $C_{\text{max}}$ , of the zero-field specific heat curves (Figure 5) for SrCuV<sub>2</sub>O<sub>7</sub> ( $C_{\text{max}} = 2.30 \text{ J K}^{-1} \text{ mol}^{-1}$ ) and BaCuV<sub>2</sub>O<sub>7</sub> ( $C_{\text{max}} = 3.16 \text{ J K}^{-1} \text{ mol}^{-1}$ ) was quite noticeable. This fact shows that the ferromagnetic intrachain interaction is affected by

(21) Belik, A. A.; Azuma, M.; Takano, M. *J. Solid State Chem.* **2004**, *177*, 883.

different  $J_2$  (if  $J_1$  is dominant) or  $J_1$  (if  $J_2$  is dominant), interchain interactions, or anisotropies.<sup>10,22</sup> In the series of isostructural 1D  $S = 1/2$  antiferromagnets, for example,  $\text{MCuP}_2\text{O}_7$  ( $M = \text{Ca}, \text{Sr}, \text{and Pb}$ ),<sup>17,18</sup> the values of  $C_{\text{max}}$  are almost the same ( $C_{\text{max}} \approx 3.0 \text{ J K}^{-1} \text{ mol}^{-1}$ ) and are consistent with the theoretical value. In addition to the broad maxima, the specific heat data also exhibited the sharp peaks at 1.36 K for  $\text{SrCuV}_2\text{O}_7$  and 1.47 K for  $\text{BaCuV}_2\text{O}_7$  because of long-range antiferromagnetic ordering (Figures 5). The  $C_p$  versus  $T$  curves for  $\text{SrCuV}_2\text{O}_7$  and  $\text{BaCuV}_2\text{O}_7$  were strongly affected by static magnetic field as for other 1D ferromagnets.<sup>3,6,8–10</sup>

A spin exchange constant,  $J$ , is expressed as  $J = J_{\text{AF}} + J_{\text{F}}$ , where  $J_{\text{AF}}$  and  $J_{\text{F}}$  are the antiferromagnetic and ferromagnetic contributions, respectively.<sup>23</sup>  $J_{\text{AF}}$  is proportional to  $OI^2$ , where  $OI$  is the overlap integral between magnetic  $x^2 - y^2$  orbitals of  $\text{Cu}^{2+}$  ions. Therefore, when  $OI$  is almost zero, the  $J_{\text{F}}$  will dominate and the spin exchange becomes ferromagnetic.

Strong dependence of the sign and strength of  $J$  values on the  $\text{Cu}-\text{O}-\text{Cu}$  bridge angle is well-known in copper dimers bridged by two  $\text{Cu}-\text{O}-\text{Cu}$  paths.<sup>24,25</sup> The exchange interaction is usually ferromagnetic for the  $\text{Cu}-\text{O}-\text{Cu}$  angle less than  $97^\circ$  and antiferromagnetic for the larger angles. However, this simple rule does not work in some compounds, for example, organic complexes containing tetranuclear or trinuclear clusters of  $\text{Cu}^{2+}$  ions.<sup>26–28</sup> In ref 28, the ferromagnetic interaction was found between  $\text{Cu}^{2+}$  ions having the  $\text{Cu}-\text{O}-\text{Cu}$  angles of  $139.2\text{--}140.5^\circ$ .

In  $\text{SrCuV}_2\text{O}_7$  and  $\text{BaCuV}_2\text{O}_7$ , the situation is more complicated because  $\text{Cu}^{2+}$  ions are connected through super-superoxide interactions,  $\text{Cu}-\text{O}\cdots\text{O}-\text{Cu}$ . The strength and sign of exchange interaction obviously depend on many parameters including bond length and angles and the nature of the chemical bonds in  $\text{TO}_4$  ( $T = \text{P or V}$ ) tetrahedra. In particular, the overlap between two  $\text{Cu}^{2+}$  magnetic orbitals associated with the  $\text{Cu}-\text{O}\cdots\text{O}-\text{Cu}$  paths depends on the overlap between two  $p$  orbitals of oxygen residing on the  $\text{O}\cdots\text{O}$  contact. Intuitively, the shorter the  $\text{O}\cdots\text{O}$  distance (i.e., the edge of  $\text{TO}_4$  tetrahedron), the larger the overlap between

$p$  orbitals.<sup>16</sup> For phosphate groups,  $\text{PO}_4^{3-}$  or  $\text{P}_2\text{O}_7^{4-}$ , the  $\text{O}\cdots\text{O}$  distance is usually  $2.5\text{--}2.55 \text{ \AA}$ . On the other hand, for vanadate groups,  $\text{VO}_4^{3-}$  or  $\text{V}_2\text{O}_7^{4-}$ , the  $\text{O}\cdots\text{O}$  distance is about  $2.7\text{--}2.8 \text{ \AA}$ . This fact can qualitatively explain why  $J$  is antiferromagnetic in such one-dimensional compounds as  $\text{SrCuP}_2\text{O}_7$ ,<sup>17</sup>  $\text{BaCuP}_2\text{O}_7$ ,<sup>18</sup> and  $(\text{VO})_2\text{P}_2\text{O}_7$ ,<sup>29</sup> while  $J$  is ferromagnetic in  $\text{SrCuV}_2\text{O}_7$  and  $\text{BaCuV}_2\text{O}_7$  despite the fact that they have similar connections between magnetic ions, that is, including  $\text{Cu}-\text{O}\cdots\text{O}-\text{Cu}$  or  $\text{V}-\text{O}\cdots\text{O}-\text{V}$  paths.

We hope that this work will encourage theoreticians to investigate the model shown in Figure 1a for (anti)ferromagnetic  $J_1$  and (anti)ferromagnetic  $J_2$  in more details. The exact quantitative description of  $\text{SrCuV}_2\text{O}_7$  and  $\text{BaCuV}_2\text{O}_7$  and determination of  $J$  values requires numerical calculations and experiments using single crystals. In particular, the first principle calculations may help to distinguish between two possibilities: (1) coupled ferromagnetic chains ( $J_1 > J_2$ ) and (2) zigzag chains with NNN interaction ( $J_2 > J_1$ ).

In conclusion, all the results obtained and the structural features of  $\text{SrCuV}_2\text{O}_7$  and  $\text{BaCuV}_2\text{O}_7$  confirm that these two compounds behave as the 1D  $S = 1/2$  ferromagnets. The typical features of 1D ferromagnets observed in  $\text{SrCuV}_2\text{O}_7$  and  $\text{BaCuV}_2\text{O}_7$  include (1) positive Weiss constant in the Curie–Weiss fitting, (2) strong field dependence of the specific heat and the real part of the ac susceptibility, (3) strong composition dependence of the value of broad maximum of the specific heat, and (4) fast saturation of the isothermal magnetization curves.  $\text{SrCuV}_2\text{O}_7$  and  $\text{BaCuV}_2\text{O}_7$  are therefore new examples in the scanty family of the 1D  $S = 1/2$  ferromagnets.

**Acknowledgment.** The authors express their thanks to the Ministry of Education, Culture, Sports, Science, and Technology, Japan, for Grants-in-Aid No. 12CE2005, for COE Research on Elements Science (No. 13440111 and No. 14204070), and for 21COE on the Kyoto Alliance for Chemistry. ICYS is supported by Special Coordination Funds for Promoting Science and Technology from MEXT, Japan.

**Supporting Information Available:** Experimental XRD patterns for  $\text{SrCuV}_2\text{O}_7$ ,  $\text{BaCuV}_2\text{O}_7$ , and  $\text{BaZnV}_2\text{O}_7$  (Figures S1–S2). TG and DTA curves for  $\text{SrCuV}_2\text{O}_7$ ,  $\text{BaCuV}_2\text{O}_7$ , and  $\text{BaZnV}_2\text{O}_7$  (Figure S3). The real part of the ac susceptibility,  $\chi'$  versus  $T$ , at different static magnetic fields for  $\text{SrCuV}_2\text{O}_7$  and  $\text{BaCuV}_2\text{O}_7$  (Figures S4 and S5). The  $C_m$  versus  $T$  and excess heat capacity curves at different static magnetic fields for  $\text{SrCuV}_2\text{O}_7$  and  $\text{BaCuV}_2\text{O}_7$  (Figures S6 and S7) (PDF). This material is available free of charge via the Internet at <http://pubs.acs.org>.

IC050164M

- (22) Campana, L. S.; Caramico D'Auria, A.; Esposito, U.; Kamieniarz, G. *Phys. Rev. B* **1989**, *39*, 9224.  
 (23) Hay, P. J.; Thibeault, J. C.; Hoffmann, R. *J. Am. Chem. Soc.* **1975**, *97*, 4884.  
 (24) Crawford, V. H.; Richardson, H. W.; Wasson, J. R.; Hodgson, D. J.; Hatfield, W. E. *Inorg. Chem.* **1976**, *15*, 2107.  
 (25) Mizuno, Y.; Tohyama, T.; Maekawa, S.; Osafune, T.; Motoyama, N.; Eisaki, H.; Uchida, S. *Phys. Rev. B* **1998**, *57*, 5326.  
 (26) Buvaylo, E. A.; Kokozay, V. N.; Vassilyeva, O. Y.; Skelton, B. W.; Jezierska, J.; Brunel, L. C.; Ozarowski, A. *Inorg. Chem.* **2005**, *44*, 206.  
 (27) Wei, M.; Willett, R. D.; Gomez-Garcia, C. J. *Inorg. Chem.* **2004**, *43*, 4534.  
 (28) Xu, Z.; Thompson, L. K.; Miller, D. O. *J. Chem. Soc., Dalton Trans.* **2002**, 2462.

- (29) Koo, H.-J.; Whangbo, M.-H.; VerNooy, P. D.; Torardi, C. C.; Marshall, W. J. *Inorg. Chem.* **2002**, *41*, 4664–4672.